DEFENCE
SCIENCE & TECHNOLOGY

Use of Spherical Objects as Calibrated Mine Hunting Sonar Targets

Stuart Anstee

DSTO-TN-0425

DEFENCE
SCIENCE & TECHNOLOGY

Use of Spherical Objects as Calibrated Minehunting Sonar Targets

Stuart Anstee

Maritime Operations Division
Aeronautical and Maritime Research Laboratory

DSTO-TN-0425

ABSTRACT

Solid, water-filled and air-filled spheres are investigated for suitability as calibrated targets for active minehunting sonars operating in the range 10kHz to 200kHz. It is found that all solid and water-filled designs have target strengths that are strongly frequency-dependent, but some air-filled designs are not frequency dependent. It is found that thick-walled spherical glass floats are suitable for some frequency ranges, and thin-walled stainless steel spheres are suitable over the whole frequency range, if they are sufficiently well made and conditions allow their deployment.

RELEASE LIMITATION

Approved for public release

Published by

DSTO Systems Sciences Laboratory
PO Box 1500
Edinburgh South Australia 5111 Australia

Telephone: (08) 8259 5555
Fax: (08) 8259 6567

AR-012-312
December 2002

APPROVED FOR PUBLIC RELEASE

Use of Spherical Objects as Calibrated Mine Hunting Sonar Targets

Executive Summary

DSTO and the RAN routinely use spherical targets for the purposes of calibrating active mine hunting sonars working in the field at frequencies above 10kHz. In some cases, the accuracy of the calibration impacts on contractual agreements. It is therefore important that the behaviour of such targets be understood, and that poor designs be avoided.

In this report, it is shown that some spherical targets that have been constructed at considerable expense for the purposes of calibrating minehunting sonars are unsuited to the purpose, because their effective target strengths vary strongly with frequency and pulse type. The "effective target strength" of an object is calculated from the largest intensity in the echo time series reflected from the object, and is appropriate to circumstances such as mine hunting where it is impossible to determine the detailed structure of an echo.

For general purposes, a mine hunting sonar target should have a well-known target strength that does not vary with frequency or pulse type. Operators should not experience a change in target strength when switching between pulse types.

It is found that:

1. Solid spheres have effective target strengths that vary strongly with frequency and pulse type.

2. Thick-walled, water-filled shells have effective target strengths that vary strongly with frequency and pulse type. The same is true of thin-walled shells.

3. Thick-walled, air-filled glass floats have effective target strengths that are approximately invariant as a function of frequency and pulse type over limited frequency ranges, but the ranges of invariance vary with thickness and must be checked experimentally.

4. Thin-walled, air-filled metal shells have effective target strengths that are approximately constant over most of the frequency range considered, so long as the bandwidth of the pulse is not extremely small.

5. Thin-walled, air-filled shells with impedances near that of water have effective target strengths that vary strongly with frequency and pulse type.

Regardless of the results of simulations, it should be stressed that objects should never be used as calibrated sonar targets without experimental verification.

Contents

1. Introduction

Well-calibrated target objects are required for the determination of active sonar detection performance. The sphere is a natural shape for such a target, since its backscattering efficiency or "target strength" does not change with aspect angle. In addition, when the radius of a sphere is much larger than the wavelength and it is constructed so that sound is not able to propagate inside it, its target strength becomes independent of frequency. This is particularly useful for a sonar target, since one unit can be used with a number of sonars.

The problem of target design is to make a spherical object with large enough target strength, which is also predictable, cheap, easily deployed, and robust.

This report discusses different designs for spherical reflectors and their performance in the frequency band 10-200kHz, which is appropriate to the detection modes of many narrowband minehunting sonars. The reflectors in question have target strengths in the neighbourhood of -20dB, since such values are appropriate to mine detection trials. The discussion is based on theoretical calculations, which predict a surprisingly wide range of phenomena, given the small number of configurations. No single design is shown to be optimal. Some designs that have been used in the past are shown to have unpredictable target strengths; others are useful over limited frequency ranges.

This report considers only "free field" target strengths, that is, target strengths of objects immersed in an infinite fluid, far from any flat surfaces. The related problem of target strength variability due to reflections from the seabed and sea surface is not considered in this work.

2. Target strength modelling

2.1 Target strength

Consider an object centred on the origin of a polar coordinate system (r,θ,ϕ). If the object is ensonified by a distant source of sound from a direction (θ,ϕ) then the sound striking the object will arrive as effectively plane waves. The intensity of backscattered sound measured by a receiver at polar coordinates (r,θ,ϕ) will depend on the shape of the object. At close range, the dependence on range r will be complicated. However, when r exceeds the "far-field" range

$$r_{ff} > \frac{L^2}{\lambda} \qquad (2.1)$$

where L is the approximate dimension of the object perpendicular to (θ,ϕ) and λ is the wavelength of the sound in the immersing fluid, then the backscattered intensity will begin to fall off simply as spherically spreading. That is, intensity I falls off as

$$I \propto \frac{1}{r^2}\exp[-\alpha(\omega)r] \tag{2.2}$$

where $\alpha(\omega)$ is the attenuation coefficient at angular frequency ω. At ranges greater than r_{ff}, we can separate out the propagation losses and talk about a range-invariant backscattering efficiency or "target strength" expressed as a function of (θ,ϕ). For convenience, target strength is expressed in terms of the intensity that would be measured at unit distance, assuming that intensity fell off like equation (2.2) at all ranges. In the frequency ranges of interest here, unit distance is 1m. Expressing target strength as a dB ratio, we have

$$TS = 10\log_{10}\left(\frac{p_r^2}{p_{inc}^2}\right) = 10\log_{10}\left(\frac{p_h^2}{p_{inc}^2}\cdot\frac{1}{r_h^2\exp(-\alpha r_h)}\right) \tag{2.3}$$

Here, p_r is the nominal backscattered pressure at unit distance, p_{inc} is the incident pressure at the origin, p_h is the pressure measured at the receiving hydrophone, which is distant $r_h > r_{ff}$ from the origin of coordinates, and α is the attenuation coefficient. The target strength is a measure of backscattering efficiency, so the source and the observer must lie on the same ray originating from the origin of the object.

Expressions (2.1)-(2.3) all apply to mono-frequency, continuous wave sound. They do not apply to pulsed systems, which are considered next.

2.1.1 Target strength for narrowband, pulsed sonars

To a very good approximation, the ocean is a non-dispersive medium for sound of moderate intensity [Urick 1983]. For a narrowband pulsed sonar system, the bandwidth B will be much smaller than the centre frequency of the pulse, and the absorption coefficient α will be approximately constant across the bandwidth of the pulse. In this case, it is appropriate to assume that equation (2.2) applies to the backscattered timeseries with f set equal to the centre frequency of the pulse. Making a second assumption that a detector (human or otherwise) will preferentially detect the most intense part of the time series, we can define the effective target strength using the maximum signal level received during the reception of the pulse.

If we assume that the detector reports the RMS average power over the duration of the pulse, then we can replace p_{inc}^2 in equation (2.3) by the expression

$$p_{\mathrm{inc}}^2 = \frac{1}{\tau}\int_0^{\tau}[p_{inc}(t)]^2\,dt \qquad (2.4)$$

where τ is the duration of the pulse. Similarly, if the backscattered waveform at the receiver is given by $p_h(t)$ and has total duration T, then we can replace p_h^2 by

$$p_h^2 = \max_{t\in[0,T-\tau]}\left\{\frac{1}{\tau}\int_t^{t+\tau}[p_h(t)]^2\right\} \qquad (2.5)$$

2.1.2 Target strength for broadband, pulsed sonars

For a broadband, pulsed sonar system, the bandwidth B of the pulse generated by the projector is of the same order as the centre frequency of the pulse. In this case, the attenuation coefficient of the medium depends non-trivially on the frequency, and equation (2.2) no longer applies to the entire pulse. In fact, the waveform leaving the projector is modified by loss of high frequency components by the time it reaches the object, and likewise, further modification occurs on the return trip to the hydrophone. Because we are now unable to separate the propagation from the scattering, there is no direct analogue to the target strength for a broadband system operating at long range from an object.

One approach that has been adopted has been to divide the pulse bandwidth into separate narrow frequency bands where expressions (2.4) and (2.5) can be applied to give a nominal target strength for each band. In sonar modelling, the same approach is applied in reverse.

More generally, let us assume that the range to the object is sufficiently large to satisfy expression (2.1) for all frequencies in the bandwidth, and sufficiently small that the higher end of the bandwidth is received with adequate signal levels. Since the transfer function of the medium is known, we will assume that an equivalent process to "pre-whitening" can be applied to the signal received by the hydrophone to remove the effects of attenuation.

If the pressure at the hydrophone is $p_h(t)$ and has Fourier transform $P_h(\omega)$, then pre-whitening could be applied in the frequency domain as

$$P_h^w(\omega) = P_h(\omega)\exp\left[\alpha(\omega)\left(r_p + r_h\right)\right] \qquad (2.6)$$

Taking the inverse Fourier transform to arrive at $p_h^w(t)$ and similarly for $p_{\mathrm{inc}}^w(t)$, we are once again able to use expressions (2.4) and (2.5) to estimate "target strength".

2.2 Target strength of a large, rigid sphere

The standard expression for the target strength a perfectly reflecting spherical scatterer is a simple expression, independent of frequency [Urick 1983]

$$TS = 10\log_{10}\left(\frac{a^2}{4}\right) \tag{2.7}$$

Here, "a" is the radius of the sphere. This expression is exact in the limit of infinite size, and is accurate within 0.3dB when

$$ka \equiv \frac{2\pi}{\lambda}a > 20 \tag{2.8}$$

This condition is fulfilled when the radius of the sphere is more than 3.2 times the wavelength. For minehunting sonars seeking proud mines[1], detection frequencies are likely to be between 10kHz and 200kHz, corresponding to wavelengths between 150mm and 7.5mm. Hence, the minimum target radius for expression (2.8) to be valid varies from 480mm at 10kHz to 24mm at 200kHz.

Table 1: Equivalent target strengths for spherical targets

TS (dB)	Equivalent radius (mm)
-10	632
-15	356
-20	200
-25	112
-30	63

Table 1 shows the radii required to provide rigid sphere targets with equivalent target strengths to a range of representative sea-mine signature levels. The size of the sphere required increases rapidly with target strength and becomes unwieldy for high target strength objects. In this work, we will consider the "low" -20dB target strength value that is often used as a standard in the literature. Even at this level, the diameter is 400mm and such a sphere is near the limit of easy storage and manual deployment.

2.3 Target strength of physically realisable spherical targets

The acoustic behaviour of a very large, rigid sphere is an ideal that can only be approached in practice. The backscattered echo from such a sphere is a replica of the incident pulse, decreased in magnitude, and appearing to come from a specular reflector at the front surface of the sphere. It will be referred to here as the "specular return". All physically realisable objects have more complicated acoustic responses.

[1] Proud in this case meaning protruding above the seabed

Solid spheres and elastic shells support families of surface waves that travel around the sphere in the water or in the elastic, each giving rise to series of evenly spaced peaks following the specular return. Solid spheres and fluid-filled shells additionally support families of interior waves that bounce around the interior. These waves have been the subject of much investigation [e.g., Hickling 1964; Gaunaurd and Werby 1987, 1991]. For the present, it suffices to say that, although they arrive after the specular return, interference effects sometimes mean that their total amplitude is larger.

As noted in Section 2.1, the target strength of an object is given by the maximum average backscattered power, which is not always the backscattered power from the specular return. This corresponds to the observational fact that a sonar operator or computer-aided detection program will probably detect the brightest part of the echo. Hence, the brightest part of the echo is used to calculate the target strength, and expression (2.5) is not valid even when it accurately predicts the power of the specular return.

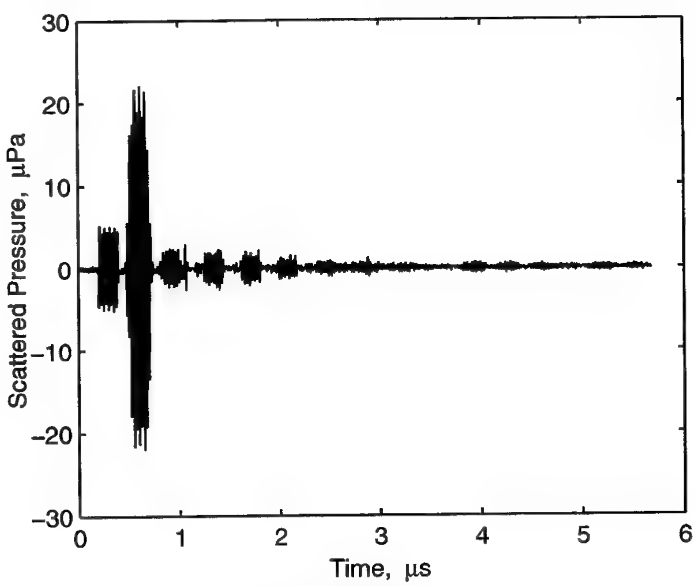

Figure 1: Theoretically calculated backscattered time series from a water-filled shell, showing the specular return from a flat toneburst pulse, followed by a series of echoes from structural waves.

Figure 1 shows the theoretically predicted backscattered waveform from a thick-walled bronze shell (shell A in Section 3.1.2) filled with water. It is ensonified by a flat, 200μs toneburst with a centre frequency of 40kHz. The specular return is the first peak in the series, and it has amplitude in agreement with the nominal target strength of the sphere, and the same shape as the incident pulse. The second and successive peaks are due to structural waves circling the sphere. They have a different shape from the incident pulse, because the structural waves are dispersive. The second peak is much

larger than the first peak, and it will consequently determine the target strength of the sphere.

2.4 Desirable target strength characteristics

In some cases, a compact target with high target strength is required. In such cases, target strength enhancement can be achieved by selecting an interacting target such as the bronze sphere considered in the previous section, or by using a "focussed" liquid-filled shell (see Section 3.1.6). However, such targets must be used with care because the effects are strongly frequency-dependent. In addition, external factors such as ambient temperature can have significant effects.

In this report, we will assume that a simple scattered waveform is desirable, implying that structural returns should be much smaller than the specular return.

2.5 Materials

The degree to which an interface between two media will transmit sound is approximately dependent on the difference between "impedances[2]", $Z_{\perp} = \rho c$ in the two media, where ρ is the density of the medium, and c is the sound speed. If there is a large mismatch, then little sound will be transmitted across the interface.

Table 2 gives values for sound speeds, densities and acoustic impedances of materials that are considered in this report [Anderson 1989; Selfidge and Pedersen[3]]. Sound speed data is scarce, restricting the choice of materials that can be accurately modelled, and the figures in the table are approximate.

Considering Table 2, we see that air has very low impedance, water, wax and nylon are intermediate and metals and glass have high impedances. Vacuum has zero impedance, and a completely rigid material has infinite impedance.

For plane interfaces, [Brekhovskikh 1980] shows that expressions for plane-wave reflection and transmission coefficients can often be put into the form

$$R = \frac{Z_2 - Z_1}{Z_2 + Z_1}; \quad T = 1 - R \tag{2.9}$$

Here, R is the plane-wave reflection coefficient and T is the plane-wave transmission coefficient. The plane wave passes from fluid 1 to medium 2. Clearly, if the two impedances are close, then transmission will be high. If they are far apart, transmission

[2] This quantity is commonly referred to as impedance. It is more accurately defined as the "specific impedance" at normal incidence [Pierce 1994].

[3] http://www.ultrasonic.com/tables/

will be low. However, even if transmission is low, sound energy can still propagate parallel to the interface as surface waves.

On a sphere, a surface wave can propagate around the circumference and radiate back at the source. If multiple waves interfere, a big secondary peak such as the one in Figure 1 can appear.

Table 2 Approximate acoustic properties of various elastic solids and fluids

Material	Longitudinal sound speed c_L (ms^{-1})	Transverse sound speed c_T (ms^{-1})	Density ρ ($kg\ m^{-3}$)	Impedance $Z_\perp$ ($kg\ m^{-2}\ s \times 10^6$)
Vacuum				0
Air	320		1	1/3000
Paraffin wax[4]	1400		900	1.3
Seawater	1500		1000	1.5
Nylon 6-6	2620	1070	1120	2.9
Glass (Pyrex)	5640	3280	2230	13
Bronze[5]	3530	2230	8860	31
Stainless steel	5790	3100	8000	46
Tungsten	5180	2870	19250	100
Ideal Rigid				Infinite

2.6 Target strength of an elastic, fluid-filled shell

2.6.1 Basic expressions

Expressions for the pressure field scattered from a spherical, fluid-filled elastic shell appear in the scientific literature as a function of frequency [Gaunaurd and Werby 1987, 1991; Readhead 1995], and they have been used in the present work to derive the target strength. Appendix A lists the expressions used. Extended expressions allowing for viscous and thermal effects have also appeared [Anson and Chivers 1993], but great care is required to avoid numerical instabilities and they have not been used here.

2.6.2 Target strength for a pulsed narrowband sonar

The expressions in Appendix A present scattered pressure as a function of frequency for a constant mono-frequency source.

[4] The sound speed is taken to equal that for paraffin oil and may be somewhat higher.
[5] Data for phosphor-bronze were used here.

In order to calculate realistic target strengths for narrowband sonars, the technique of Fourier reconstruction [e.g., Jensen et al, 1994] has been used to generate backscattered timeseries for narrowband pulses. Figure 1 is an example of this. The target strength is then calculated according to expression (2.3), as the maximum mean-square ratio of backscattered to incident intensity along the timeseries, where the mean is taken over the duration of the incident pulse.

In the following sections, target strength is presented both as a function of frequency, and as a function of the centre frequency of toneburst pulses of 100μs and 200μs duration.

2.6.3 Target strength and pulse compression

The use of pulse compression processing, where the received signal is cross-correlated with a replica of the emitted wideband pulse, would cause further variation to the apparent target strength. However, given that surface-wave propagation is dispersive, it is likely that the replicate correlator would suppress returns due to structure-borne sound. The specular return, for which expression (2.7) is usually a good approximation, would then be favoured. In general, target strength should be reassessed separately for each pulse type and signal processing chain.

3. Assessment of some designs for sonar targets

3.1 Designs

The problem of fabricating spherical targets is not trivial. Glass spheres break easily and thin metal shells are easily dented and crushed. Thick shells and solid spheres are typically very heavy. Making an object accurately spherical is difficult and it must be robust enough to maintain its shape after multiple episodes of handling and deployment.

In addition, the sphere should be separated from the seabed by a few radii in order to avoid changes in the target strength due to interference between directly reflected sound and sound bounced from the seabed underneath the target [Bishop and Smith 1999]. At long ranges, further changes to apparent target strength occur due to interference between direct backscatter and multipaths arriving at similar angles. The multipaths arrivals have made one or more intermediate bounces from the seabed or sea surface. They are not true backscatter, but the vertical directivity of most minehunting sonars is insuffient to suppress them. Multipath effects are not considered further in this report.

hunting sonars is insufficient to suppress them. Multipath effects are not considered further in this report.

3.1.1 Solid spheres

A solid elastic sphere is the simplest spherical target, but in most cases it is not a good design, because it is excessively heavy, difficult to suspend above the seabed and the target strength varies with frequency.

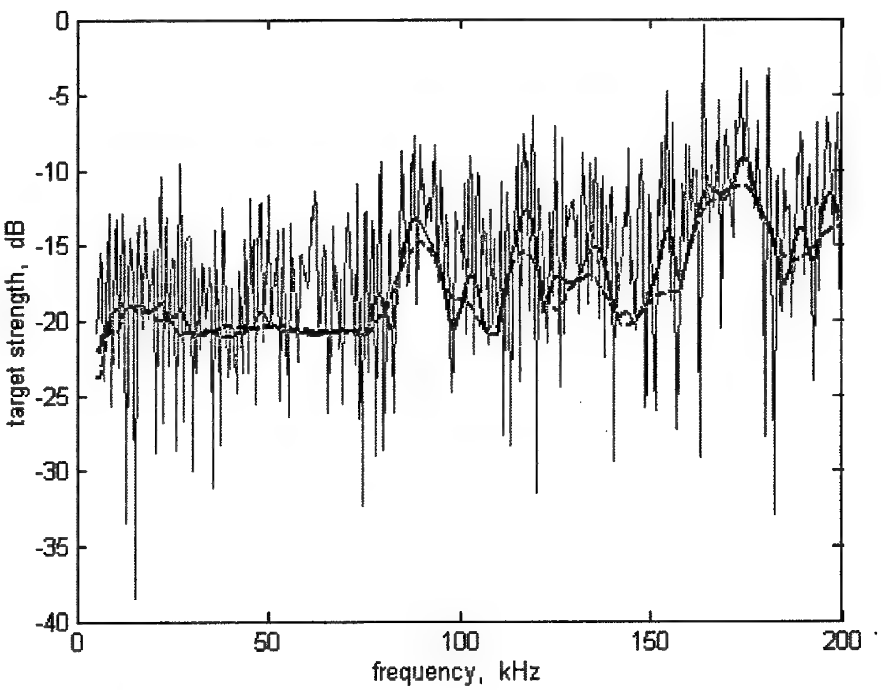

Figure 2 Target strength of a 400mm diameter bronze sphere. Target strength of equivalent rigid sphere is –20dB.

Figure 2 shows the predicted target strength of a solid bronze sphere, insonified with a constant pure tone (thin, grey line), a 200μs toneburst pulse (thick, blue, solid line) and a 100μs pulse (thick, red, dashed line). In the first case, the frequency is that of the tone[6], and in the latter two cases it is the centre frequency of the pulse. The diameter of the sphere is 400mm and the target strength of an equivalent rigid sphere is –20dB.

The variation of target strength for the pure tone shows numerous peaks and nulls due to structural waves. The complicated curve is typical for strongly interacting structures.

[6] This corresponds to the frequency response of the target.

The variation of target strength for both pulses is smoother, since their frequency spreads act to average over individual peaks and nulls. The 100μs curve approaches the rigid-sphere value (-20dB) in the 30-70kHz range, but departs from it significantly elsewhere, especially at higher frequencies.

From Table 2, it can be seen that bronze has only 30% of the impedance of tungsten, which has the highest impedance of commonly available materials. When the material parameters of tungsten were adopted, the variation of target strength within the frequency range was lower than for bronze, but the same general pattern was observed.

Summary: Solid metal or glass spheres are not suitable as mine hunting sonar targets.

3.1.2 Water-filled, thick-walled shells

In the past, thick-walled, water-filled shells were fabricated and used as sonar targets. They were designed using expression (2.1), neglecting structural effects. The shells were designed to flood when placed underwater, since it made them much easier to deploy than a buoyant, air-filled sphere. Four sizes of sphere were cast in aluminium bronze, and their exteriors were machined spherical to narrow tolerances. Details are given in Table 3.

Table 3 Characteristics of bronze spheres

Name	Shell material	Outer diameter (mm)	Wall thickness (mm)	Approx weight (kg)	Nominal target strength (dB)
A	AB2[7]	210	12-16	17	-25.6
B	AB2	330	12-16	42	-21.7
C	AB2	430	12-16	72	-19.4
D	AB2	650	12-16	165	-15.8

Figures 3 and 4 show target strengths calculated for each sphere, water-filled. The curves are for a constant pure tone (thin line), a 100μs toneburst (thick, dashed line) and a 200μs toneburst (thick, solid line). It is immediately obvious that the target strengths of the spheres are strongly affected by structural effects when they are water-filled. Their target strengths do not agree with the nominal values in Table 3, and the increase in target strength with radius is not monotonic at most frequencies, although it is present as an overall trend.

[7] AB2 is Nickel Aluminium Bronze alloy, a marine alloy defined in British Standard BS1400 as "AB2".

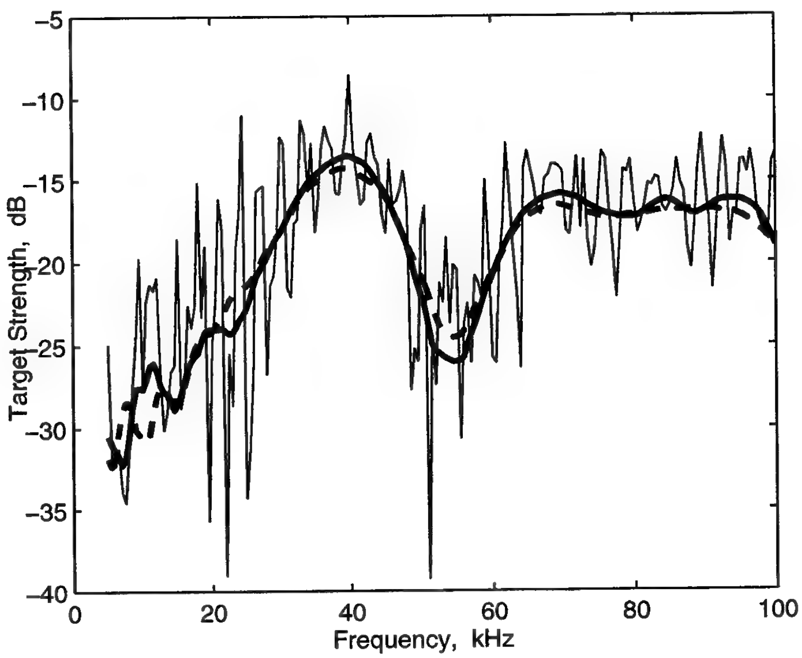

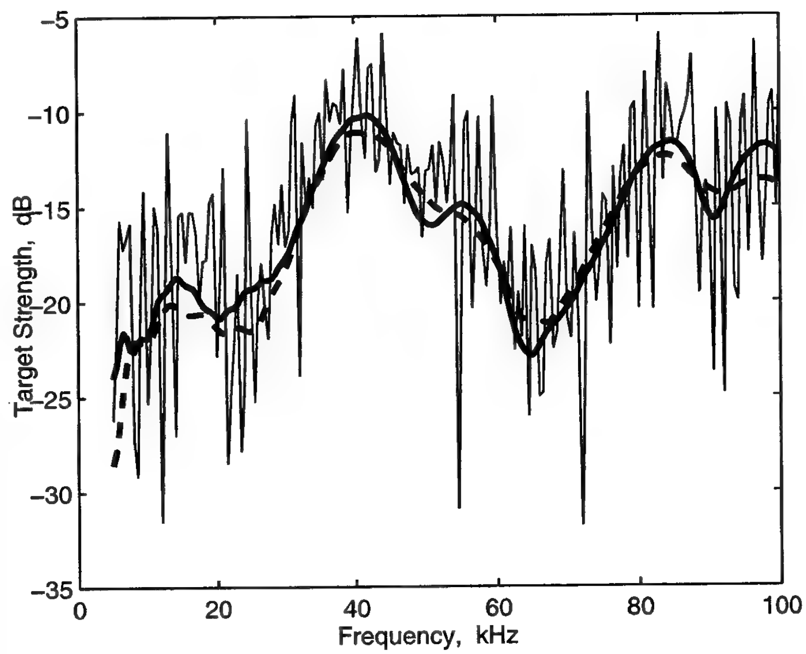

Figure 3: Target strengths for bronze shells A (top) and B (bottom), when water-filled.

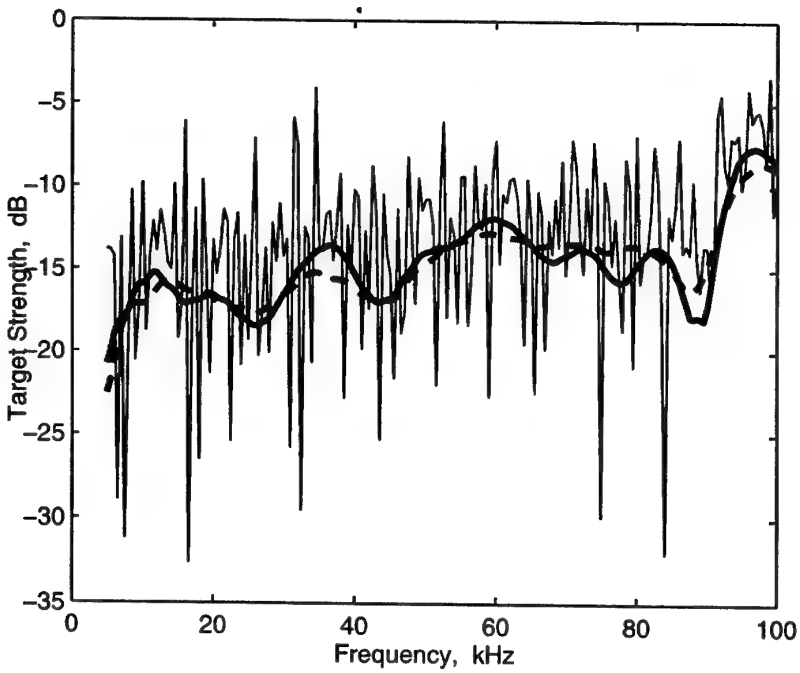

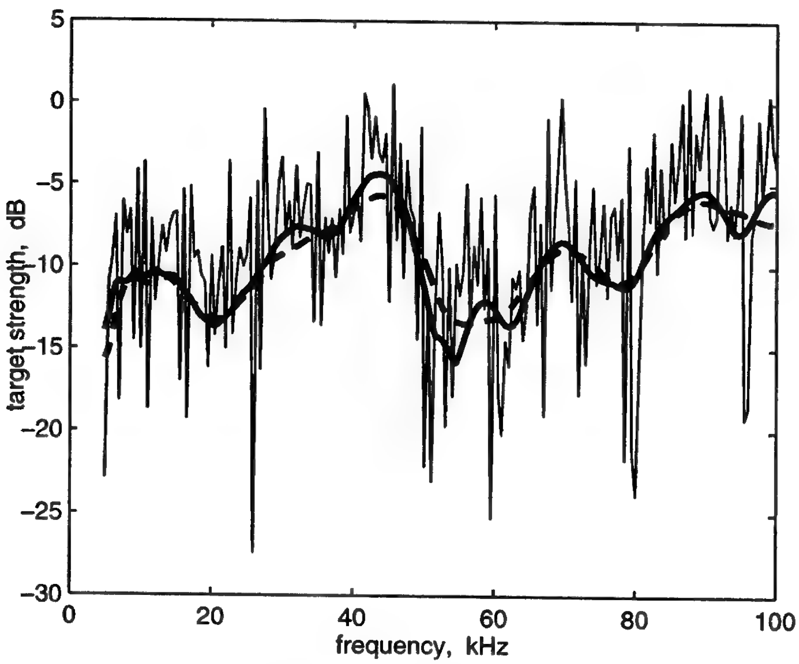

Figure 4 Target strengths for the bronze shells C (top) and D (bottom), when water-filled.

3.1.3 Air-filled thick-walled shells

Figure 5, which shows the target strength of shell D when air-filled, is quite different to the corresponding plot in Figure 4. In this case, structural interactions still occur, but they are modified because the waves propagating in the shell cannot radiate into the interior. Both the pure-tone and pulse target strengths are much simpler curves than in the water-filled case, and the pulse target strengths are in good agreement with the nominal target strength for frequencies greater than 55kHz. However, there is still a strong effect due to propagation within the shell.

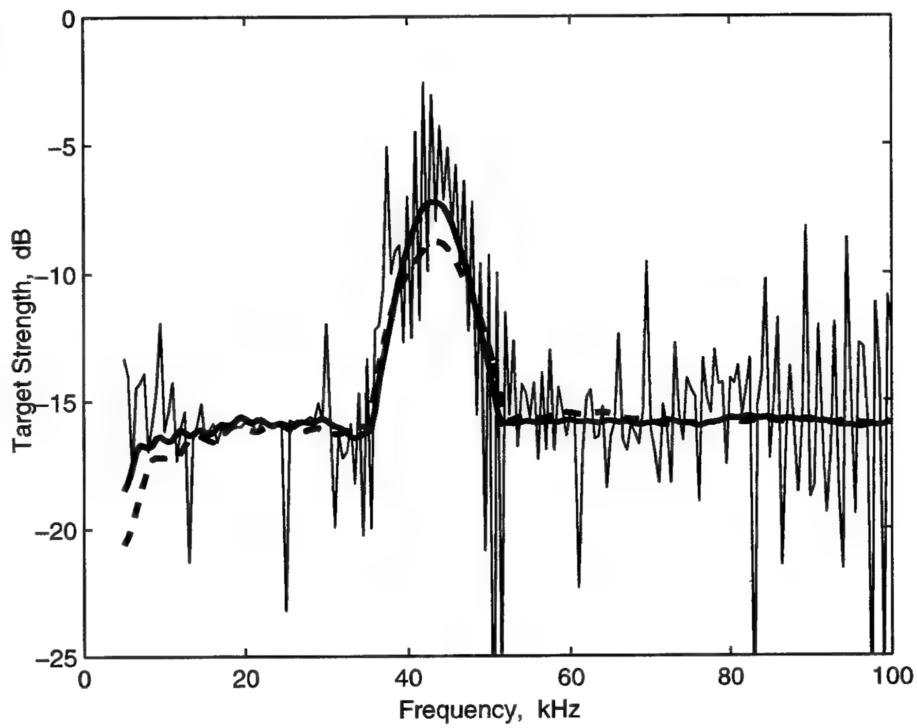

Figure 5 Target strengths for the bronze shell D, when air filled

3.1.3.1 Glass spheres

Figure 6 shows calculated target strengths for a family of air-filled spherical shells of different thicknesses. All results are for 200μs pulses. The thickness has been varied between 5mm and 20mm in 5mm steps.

The nominal target strength of the spheres is -20dB, which is in good agreement with the calculated target strength for each configuration over much of the frequency range. However, at least one resonant peak appears in each curve and it is clear that care must be exercised when using these spheres. The target strength should be measured at and

around each frequency of interest in order to establish that the sphere is not in a resonant frequency range.

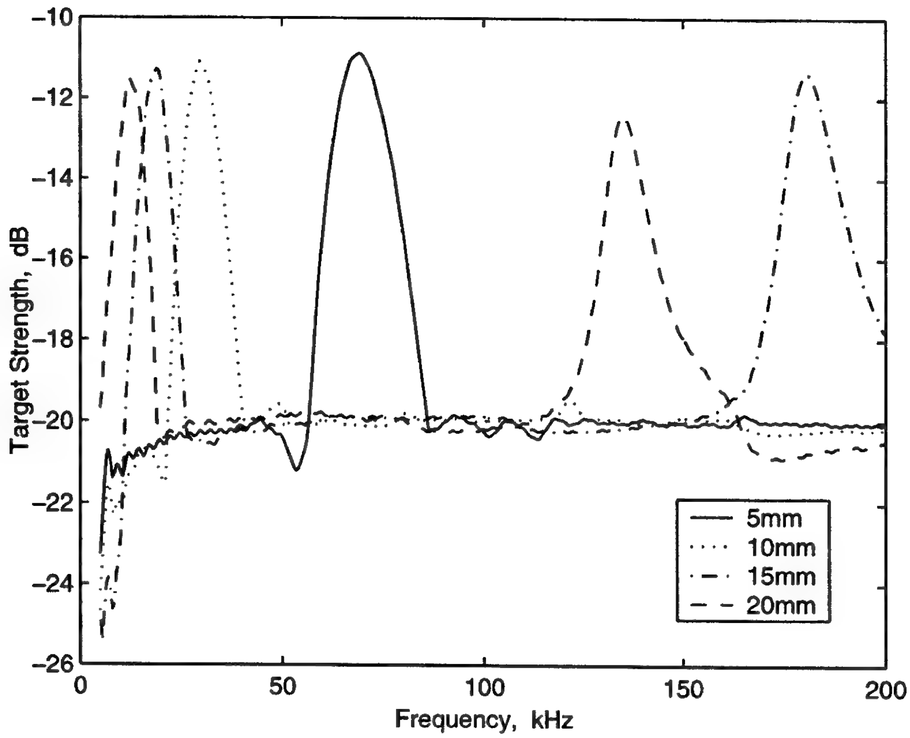

Figure 6 Target strength of borosilicate glass (Pyrex) spheres of 400mm diameter and various thicknesses.

3.1.3.2 *Benthos glass shells*

Thick-walled, air-filled borosilicate glass spheres are available from Benthos Corporation[8], where they are sold as deep sea floatation devices. They have been used for numerous sonar trials. The glass shells are spherical to high accuracy to withstand extreme pressures, and evacuated to 0.3 atmospheres to ensure that their two halves stay together on the surface. The diameter of the largest sphere is 432mm or 17″ and the wall thickness is 15.9mm or 5/8″.

The nominal target strength of the 17″ sphere is nominally -19dB, and its variation with frequency closely follows the 15mm thickness curve of Figure 6. [Wyber 2001] has conducted measurements of the target strength in the frequency range 22-50kHz. He finds that the theoretical and measured target strengths are in close agreement, including the peak predicted at frequencies under 30kHz. He also finds that when the

[8] http://www.benthos.com

conducted measurements of the target strength in the frequency range 22-50kHz. He finds that the theoretical and measured target strengths are in close agreement, including the peak predicted at frequencies under 30kHz. He also finds that when the target strength of the specular return is considered alone, it varies within 1dB of the rigid-sphere value.

3.1.4 Manufacturing thin-walled shells

Thin-walled shells for maritime use are necessarily made from either plastic or metal. The wall thickness is much less than a wavelength in order to minimise the acoustic interaction between the incident pulse and the shell material.

3.1.4.1 Thin-walled metal shells

Thin-walled metal shells are fabricated in two stages. Separate halves are "spun" or pressed from thin sheet metal, and then the halves are welded together.

Stainless steel shells were fabricated for DSTO in sizes up to 305mm diameter over a period of years. The nominal wall thickness of the shells was 0.8mm, but probably varied significantly. All of the shells were somewhat distorted due to the manufacturing process. In addition, they were equipped with stopcocks to enable fluid-loading and carrying lugs, which could be expected to have an effect on the target strength. In general, the shells are easily dented, and they probably could not be deployed air-filled in a high-pressure deep-water environment[9].

3.1.4.2 Thin-walled plastic shells

Thin-walled plastic shells are an option for shallow-water deployment, providing the expense of manufacture is acceptable. The fabrication of a mold is expected to be extremely expensive, after which the production costs are cheap. Plastic shells can be manufactured to very high tolerances and should have aspect-independent target strengths.

3.1.5 Air-filled thin-walled shells

3.1.5.1 Stainless steel shells

Assuming that a stainless steel shell could be made with a diameter of 400mm, the top half of Figure 7 shows the target strength predictions for such a target. The pure-tone target strength (thin line) fluctuates between resonant peaks and troughs, but the value oscillates around the nominal value of –20dB and this is reflected in the 200μs pulse curve (thick line), which varies within a 1dB range for frequencies over 30kHz.

[9] Pressurization may be an option in this case, since the impedance mismatch with water remains high as pressure is increased.

It is concluded that air-filled thin-walled stainless steel shells are a viable option, provided they can be made large enough to have the desired target strength (Table 1).

3.1.5.2 *Plastic shells*

Most plastics have impedance values close to that of water and hence it could be expected that a plastic shell would have little impact on the target strength. As an example, we assume that a 400mm diameter, air-filled nylon shell could be manufactured with a 3mm wall thickness. The bottom half of Figure 7 shows the target strength predictions. Rather than being better than the stainless-steel shell, the nylon shell is worse, as the target strength varies greatly with frequency. Changing the thickness of the shell did not improve the behaviour, so it would appear that this approach is not viable.

3.1.6 Fluid-filled, focussed thin shells

The difficulty of making and deploying large, air-filled spheres with very large buoyancy has prompted several workers [Folds 1971; Marks and Mikeska 1976; Readhead 1995; Kaduchak and Loeffler 1998; Deveau 2000, 2001] to attempt to enhance target strengths by selecting an appropriate fill fluid. When the sound speed of the fluid causes sound entering the front face of the sphere to be focussed on the back wall of the sphere, the backscattering efficiency increases dramatically, so much smaller spheres can be used to achieve a given target strength.

The operational experience with focussed shells made by DSTO has been that the target strengths appear to fluctuate over a wider range than is desirable for sonar trials. Part of this variation may be explained by shifts in target strength with frequency, temperature and the sphere parameters, as discussed by [Readhead 1995]. It is also possible that distortions in the shell had a large effect on the target strength at some aspect angles, or that multipath interference is important.

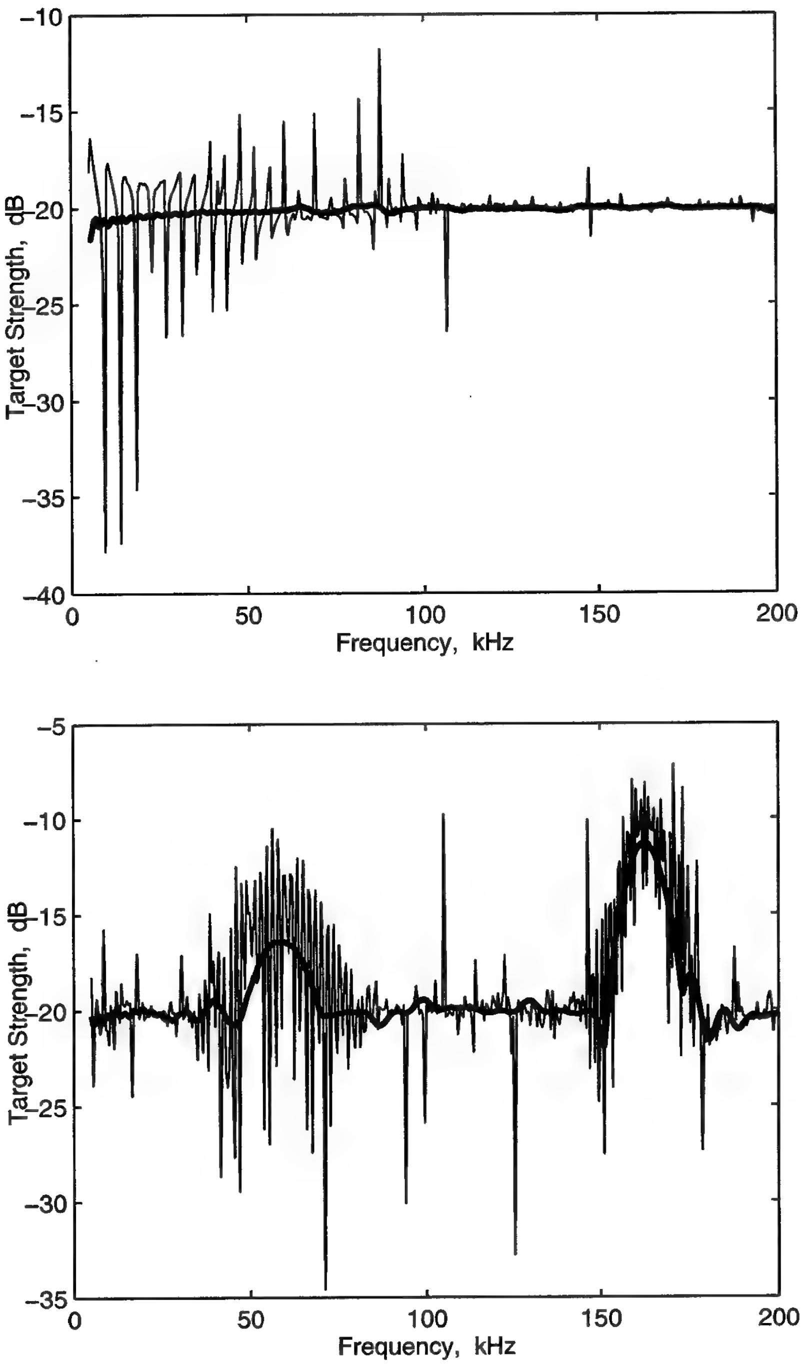

Figure 7: Target strengths of 400mm diameter, air-filled stainless steel (top) and nylon (bottom) shells

Summary: Focussed spheres are no longer used for sonar trials by the RAN, since target strength appeared to fluctuate considerably. Further work is required to determine the conditions under which they should be used. If used, they must be characterised for the conditions prevailing during the trial.

3.2 Deployment

Deployment of spherical targets introduces additional complications.

Negatively buoyant spheres are placed on the bottom and remain there. Their apparent target strengths are affected (usually increased) by the proximity of the seabed ground plane. While it could be argued that the change in target strength mimics the change to the target strength of a ground mine measured in mid-water, the effect is difficult to predict. Unfortunately, the obvious remedy of raising the sphere several diameters above the bottom does not remove all fluctuations. Multiple bounces between the sphere and the seabed are eliminated, but distant multipaths are not. This is a topic for further research. Note also that, if a float or a stand is used to elevate the sphere, its target strength must be taken into account.

Air-filled spheres may exert large buoyancy forces. For example, the Benthos glass targets experience a buoyance force of 25.4 kg weight. Hence, they must be tethered to the seabed with a weight or other fixture. The weight must be designed to have much lower target strength than the sphere, and it must not scatter sound directly at the sphere it is tethering.

4. Conclusions

In this report, different designs for spherical targets have been examined, and some examples have been considered in detail. All of the designs have a narrowband pulse target strength that varies with frequency, with the sole exception of the thin-walled, air-filled stainless steel sphere.

In summary:

1. Solid spheres have effective target strengths that vary with frequency and pulse type.

2. Thick-walled, water-filled shells have effective target strengths that vary with frequency and pulse type.

3. Thick-walled, air-filled glass floats have effective target strengths that are invariant with frequency over limited frequency ranges, but the frequency

ranges for which invariance holds vary with wall thickness and must be checked experimentally.

4. Thin-walled, air-filled metal shells have effective target strengths that do not vary strongly with frequency for narrowband pulse types. Fabrication and deployment difficulties are an important limitation.

5. Thin-walled, air-filled shells with shell impedances near that of water have effective target strengths that vary with frequency and pulse type.

Regardless of the results of simulations, it should be stressed that objects should never be used as calibrated sonar targets without experimental verification.

5. References

Abramowitz, M. and Stegun, I. A. (1964) *Handbook of mathematical functions,* Dover.

Anderson, H. L. (1989) *A physicist's desk reference. The second edition of Physics Vade Mecum,* American Insitute of Physics, New York.

Anson, L. W. and Chivers, R. C. (1993) Ultrasonic scattering from spherical shells including viscous and thermal effects, *J. Acoustic. Soc. Am.*, **93**(4), Pt. 1, 1687-1699.

Brekhovskikh, L. M. (1980) *Waves in Layered Media*, Academic Press, New York.

Gaunaurd, G. C. and Werby, M. F. (1987) Lamb and creeping waves around submerged spherical shells resonantly excited by sound scattering, *J. Acoustic. Soc. Am.*, **82**(6), 2021-2033.

Gaunaurd, G. C. and Werby, M. F. (1991) Sound scattering by resonantly excited, fluid-loaded, elastic spherical shells, *J. Acoustic. Soc. Am.*, **90**(5), 2536-2550.

Hickling, R. (1964) Analysis of echoes from a hollow metallic sphere in water, *J. Acoustic. Soc. Am.*, **36**(6), 1124-1137.

Jensen, F. B., Kuperman, W. A., Porter, M. B. and Schmidt, H. (1994) *Computational Ocean Acoustics*, Springer-Verlag.

Kaduchak, G. and Loeffler, C. M. (1998) Relationship between material parameters and target strength of fluid-filled spherical shells in water: calculations and observations, *IEEE J. Oceanic Eng.,* **23**(1), 26-30.

Pierce, A. D. (1994) *Acoustics – An introduction to its physical principles and applications, 3rd Edition,* American Institute of Physics Press.

Readhead, M. L. (1995) *Calculations of the sound scattering from fluid-filled spherical shell sonar targets*, DSTO Research Report DSTO-RR-0020, DSTO Aeronautical and Maritime Research Laboratory, P.O. Box 4331, Melbourne Vic 3001, Australia.

Urick, R. J. (1983) *Principles of underwater sound, 3rd Edition.* McGraw-Hill, New York.

6. Acknowledgements

The author wishes to acknowledge the extensive assistance provided by Dr Mark Readhead of DSTO, who contributed advice, assistance with debugging and his own code for Bessel functions of large order and argument. The author also wishes to acknowledge the contributions of the referee in clarifying the work.

This work was done in support of the Acceptance Into Naval Service process for the Royal Australian Navy Mine Hunter Coastal.

Appendix A: Expressions for scattered pressure

The expressions for scattered pressure appearing in [Readhead 1995] were used in this work, however they contained a misprint[10], so they are reproduced here in corrected form. It was also decided to adopt the convention $\exp(-i\omega t)$ for propagating waves, in agreement with the bulk of the scattering literature.

Let the frequency be *f*, and define wavenumbers

$$
\begin{aligned}
k_1 &= \frac{2\pi f}{c_1} && \text{(outer fluid)} \\
k_L &= \frac{2\pi f}{c_L}; \quad k_T = \frac{2\pi f}{c_T} && \text{(shell - longitudinal and transverse)} \qquad \text{(A.1)} \\
k_3 &= \frac{2\pi f}{c_3} && \text{(inner fluid)}
\end{aligned}
$$

Here, c_1 and c_3 are respectively the sound speeds in the outer and inner fluids, and c_L and c_T are respectively the longitudinal and transverse elastic wave speeds in the shell material.

The outer radius of the shell is *a* and the inner radius is *b*.

Assume the projector is a point source. Let the pressure at range *R* from the projector be defined by

$$p_i = P_0 \frac{e^{+ik_1 R}}{R} \qquad \text{(A.2)}$$

Now, let the origin of coordinates be the centre of the sphere, and let the projector be located at range r_p along the negative z-axis. Assume that the receiver is located at polar coordinates (r_r, θ_r) then the scattered pressure for a receiver located closer to the origin than the projector is given by

$$p_s = P_0 k_1 \sum_{l=0}^{\infty} (-1)^l (2l+1) C_l \mathrm{h}_l^{(1)}(k_1 r_p) \mathrm{h}_l^{(1)}(k_1 r_r) \mathrm{P}_l(\cos\theta_r) \quad \text{for } a < r_r < r_p \qquad \text{(A.3)}$$

Here, $h_l^{(1)}(x)$ is the *l*-th order spherical Hankel function of the first kind [Abramowitz and Stegun 1964], and $P_l(x)$ is the *l*-th order Legendre polynomial.

10 The misprint was not present in computer codes and did not affect the calculations shown in the report.

The coefficients C_l are given by the ratio of determinants

$$C_l = \mathrm{i}\frac{\begin{vmatrix} \gamma_{11} & \gamma_{12} & \gamma_{13} & \gamma_{14} & g_1 & 0 \\ \gamma_{21} & \gamma_{22} & \gamma_{23} & \gamma_{24} & 0 & \gamma_{26} \\ \gamma_{31} & \gamma_{32} & \gamma_{33} & \gamma_{34} & g_3 & 0 \\ \gamma_{41} & \gamma_{42} & \gamma_{43} & \gamma_{44} & 0 & \gamma_{46} \\ \gamma_{51} & \gamma_{52} & \gamma_{53} & \gamma_{54} & 0 & 0 \\ \gamma_{61} & \gamma_{62} & \gamma_{63} & \gamma_{64} & 0 & 0 \end{vmatrix}}{\begin{vmatrix} \gamma_{11} & \gamma_{12} & \gamma_{13} & \gamma_{14} & \gamma_{15} & 0 \\ \gamma_{21} & \gamma_{22} & \gamma_{23} & \gamma_{24} & 0 & \gamma_{26} \\ \gamma_{31} & \gamma_{32} & \gamma_{33} & \gamma_{34} & \gamma_{35} & 0 \\ \gamma_{41} & \gamma_{42} & \gamma_{43} & \gamma_{44} & 0 & \gamma_{46} \\ \gamma_{51} & \gamma_{52} & \gamma_{53} & \gamma_{54} & 0 & 0 \\ \gamma_{61} & \gamma_{62} & \gamma_{63} & \gamma_{64} & 0 & 0 \end{vmatrix}} \tag{A.4}$$

The non-zero matrix coefficients appearing in (A.4) are listed below

$$\gamma_{11} = \frac{\sigma}{1-2\sigma}(k_L a)^2 \mathrm{j}_l(k_L a) - (k_L a)^2 \mathrm{j}_l''(k_L a) \tag{A.5}$$

$$\gamma_{12} = \frac{\sigma}{1-2\sigma}(k_L a)^2 \mathrm{n}_l(k_L a) - (k_L a)^2 \mathrm{n}_l''(k_L a) \tag{A.6}$$

$$\gamma_{13} = l(l+1)\mathrm{j}_l(k_T a) - l(l+1)k_T a\, \mathrm{j}_l'(k_T a) \tag{A.7}$$

$$\gamma_{14} = l(l+1)\mathrm{n}_l(k_T a) - l(l+1)k_T a\, \mathrm{n}_l'(k_T a) \tag{A.8}$$

$$\gamma_{15} = \frac{(k_T a)^2}{2\rho_2}\mathrm{h}_l^{(1)}(k_1 a) \tag{A.9}$$

$$\gamma_{21} = \frac{\sigma}{1-2\sigma}(k_L b)^2 \mathrm{j}_l(k_L b) - (k_L b)^2 \mathrm{j}_l''(k_L b) \tag{A.10}$$

$$\gamma_{22} = \frac{\sigma}{1-2\sigma}(k_L b)^2 \mathrm{n}_l(k_L b) - (k_L b)^2 \mathrm{n}_l''(k_L b) \tag{A.11}$$

$$\gamma_{23} = l(l+1)\mathrm{j}_l(k_T b) - l(l+1)k_T b\, \mathrm{j}_l'(k_T b) \tag{A.12}$$

$$\gamma_{24} = l(l+1)\mathrm{n}_l(k_T b) - l(l+1)k_T b\,\mathrm{n}_l'(k_T b) \tag{A.13}$$

$$\gamma_{26} = \frac{(k_T b)^2}{2\rho_2}\mathrm{j}_l(k_3 b) \tag{A.14}$$

$$\gamma_{31} = k_L a\,\mathrm{j}_l'(k_L a) \tag{A.15}$$

$$\gamma_{32} = k_L a\,\mathrm{n}_l'(k_L a) \tag{A.16}$$

$$\gamma_{33} = l(l+1)\mathrm{j}_l(k_T a) \tag{A.17}$$

$$\gamma_{34} = l(l+1)\mathrm{n}_l(k_T a) \tag{A.18}$$

$$\gamma_{35} = \frac{k_1 a}{\rho_1}\mathrm{h}_l'^{(1)}(k_1 a) \tag{A.19}$$

$$\gamma_{41} = k_L b\,\mathrm{j}_l'(k_L b) \tag{A.20}$$

$$\gamma_{42} = k_L b\,\mathrm{n}_l'(k_L b) \tag{A.21}$$

$$\gamma_{43} = l(l+1)\mathrm{j}_l(k_T b) \tag{A.22}$$

$$\gamma_{44} = l(l+1)\mathrm{n}_l(k_T b) \tag{A.23}$$

$$\gamma_{46} = \frac{k_3 b}{\rho_3}\mathrm{j}_l'(k_3 b) \tag{A.24}$$

$$\gamma_{51} = 2k_L a\,\mathrm{j}_l'(k_L a) - 2\mathrm{j}_l(k_L a) \tag{A.25}$$

$$\gamma_{52} = 2k_L a\,\mathrm{n}_l'(k_L a) - 2\mathrm{n}_l(k_L a) \tag{A.26}$$

$$\gamma_{53} = (k_T a)^2\,\mathrm{j}_l''(k_T a) + [l(l+1)-2]\mathrm{j}_l(k_T a) \tag{A.27}$$

$$\gamma_{54} = (k_T a)^2\,\mathrm{n}_l''(k_T a) + [l(l+1)-2]\mathrm{n}_l(k_T a) \tag{A.28}$$

$$\gamma_{61} = 2k_L b\,\mathrm{j}_l'(k_L b) - 2\mathrm{j}_l(k_L b) \tag{A.29}$$

$$\gamma_{62} = 2k_L b\,\mathrm{n}_l'(k_L b) - 2\mathrm{n}_l(k_L b) \tag{A.30}$$

$$\gamma_{63} = (k_T b)^2\,\mathrm{j}_l''(k_T b) + [l(l+1)-2]\,\mathrm{j}_l(k_T b) \tag{A.31}$$

$$\gamma_{64} = (k_T b)^2\,\mathrm{n}_l''(k_T b) + [l(l+1)-2]\,\mathrm{n}_l(k_T b) \tag{A.32}$$

The numerator is identical to the denominator except for the substituted coefficients

$$g_1 = \frac{(k_T a)^2}{2\rho_2}\,\mathrm{j}_l(k_1 a) \tag{A.33}$$

$$g_3 = \frac{k_1 a}{\rho_1}\,\mathrm{j}_l'(k_1 a) \tag{A.34}$$

Here, $j_l(x)$ and $n_l(x)$ are the *l*-th order spherical Bessel and Neumann functions, ρ_1, ρ_2 and ρ_3 are the densities of the outer fluid, shell and inner fluid respectively, *a* and *b* are the outer and inner shell radii, and σ is Poisson's ratio for the shell. The symbols *a* and *b* have been interchanged from Readhead's convention to reflect the usage in the general literature. Equations (A.27), (A.28), (A.31) and (A.32) have been corrected.

DISTRIBUTION LIST

Use of Spherical Objects as Calibrated Mine Hunting Sonar Targets

Stuart Anstee

AUSTRALIA

DEFENCE ORGANISATION

Task Sponsor

COMAUSNAVMCDGRP
DDMWD
SODEV POL (LCDR Steve Bliss, HMAS Waterhen)

MHCOTD (CMDR Paul Hornsby, Building 89, Garden Island)
OPSUPO (LCDR Russ Crawford, HMAS Waterhen)
Test & Trials Manager, MHC Project
(Matthew Clarkson, R2-3-C043, Canberra)
MHSD (LCDR Peter Johnson, Hydrographic Office)

S&T Program

Chief Defence Scientist
FAS Science Policy
AS Science Corporate Management
Director General Science Policy Development
} shared copy
Counsellor Defence Science, London (Doc Data Sheet)
Counsellor Defence Science, Washington (Doc Data Sheet)
Scientific Adviser to MRDC Thailand (Doc Data Sheet)
Scientific Adviser Joint
Navy Scientific Adviser
Scientific Adviser - Army (Doc Data Sheet and distribution list only)
Air Force Scientific Adviser
Director Trials

Director AMRL

Chief of Maritime Operations Division

DSTO Pyrmont

Dr Alan Theobald
Dr Brian Ferguson
Dr Stuart Anstee
Dr Ping Cao
Dr Mark Readhead
Ms Jane Cleary
Dr Ranjit Thuraisingham

MOD Edinburgh
- Dr Adrian Jones
- Dr Yong Zhang
- Mr Robert Dow

MPD Maribyrnong
- Dr Ian MacGillivray

DSTO Library and Archives
- Library Edinburgh
- Australian Archives
- Library, MOD, Pyrmont
- US Defense Technical Information Center, 2 copies
- UK Defence Research Information Centre, 2 copies
- Canada Defence Scientific Information Service, 1 copy
- NZ Defence Information Centre, 1 copy
- National Library of Australia, 1 copy

Capability Systems Staff
- Director General Maritime Development
- Director General Aerospace Development (Doc Data Sheet only)

Knowledge Staff
- Director General Command, Control, Communications and Computers (DGC4) (Doc Data Sheet only)

Navy
- SO (SCIENCE), COMAUSNAVSURFGRP, BLD 95, Garden Island, Locked Bag 12, PYRMONT NSW 2009 (Doc Data Sheet and distribution list only)

Army
- ABCA National Standardisation Officer (4 copies)
  Land Warfare Development Sector
  Tobruk Barracks
  PUCKAPUNYAL VIC 3662
- SO (Science), Deployable Joint Force Headquarters (DJFHQ) (L), MILPO Gallipoli Barracks, Enoggera QLD 4052 (Doc Data Sheet only)

Intelligence Program
- DGSTA Defence Intelligence Organisation
- Manager, Information Centre, Defence Intelligence Organisation

Corporate Support Program
- Library Manager, DLS-Canberra
- Defence Library Service - Sydney West (Doc Data Sheet)

UNIVERSITIES AND COLLEGES
- Australian Defence Force Academy
  - Library
  - Head of Aerospace and Mechanical Engineering
- Hargrave Library, Monash University (Doc Data Sheet only)

Librarian, Flinders University

OTHER ORGANISATIONS
NASA (Canberra)
AusInfo

OUTSIDE AUSTRALIA

ABSTRACTING AND INFORMATION ORGANISATIONS
Library, Chemical Abstracts Reference Service
Engineering Societies Library, US
Materials Information, Cambridge Scientific Abstracts, US
Documents Librarian, The Center for Research Libraries, US

INFORMATION EXCHANGE AGREEMENT PARTNERS
Acquisitions Unit, Science Reference and Information Service, UK
Library - Exchange Desk, National Institute of Standards and Technology, US

SPARES (5 copies)

Total number of copies: 61

DEFENCE SCIENCE AND TECHNOLOGY ORGANISATION DOCUMENT CONTROL DATA				
			1. PRIVACY MARKING/CAVEAT (OF DOCUMENT)	
2. TITLE Use of Spherical Objects as Calibrated Mine Hunting Sonar Targets		3. SECURITY CLASSIFICATION (FOR UNCLASSIFIED REPORTS THAT ARE LIMITED RELEASE USE (L) NEXT TO DOCUMENT CLASSIFICATION) Document (U) Title (U) Abstract (U)		
4. AUTHOR(S) Stuart Anstee		5. CORPORATE AUTHOR Systems Sciences Laboratory PO Box 1500 Edinburgh South Australia 5111 Australia		
6a. DSTO NUMBER DSTO-TN-0425	6b. AR NUMBER AR-012-312	6c. TYPE OF REPORT Technical Note	7. DOCUMENT DATE December 2002	
8. FILE NUMBER 490/6/122	9. TASK NUMBER NAV 00/037	10. TASK SPONSOR COMAUSNAVMCDGRP	11. NO. OF PAGES 24	12. NO. OF REFERENCES 12
13. URL on the World Wide Web http://www.dsto.defence.gov.au/corporate/reports/DSTO-TN-0425.pdf			14. RELEASE AUTHORITY Chief, Maritime Operations Division	
15. SECONDARY RELEASE STATEMENT OF THIS DOCUMENT Approved for public release OVERSEAS ENQUIRIES OUTSIDE STATED LIMITATIONS SHOULD BE REFERRED THROUGH DOCUMENT EXCHANGE, PO BOX 1500, EDINBURGH, SA 5111				
16. DELIBERATE ANNOUNCEMENT No Limitations				
17. CASUAL ANNOUNCEMENT Yes				
18. DEFTEST DESCRIPTORS Sound scattering; Sonar; Calibrating; Spherical Shell; Sonar Transmission (Pulsed); Sonar Targets; Sound Pressure; Acoustic Measurement				

19. ABSTRACT

Solid, water-filled and air-filled spheres are investigated for suitability as calibrated targets for active minehunting sonars operating in the range 10kHz to 200kHz. It is found that all solid and water-filled designs have target strengths that are strongly frequency-dependent, but some air-filled designs are not frequency dependent. It is found that thick-walled spherical glass floats are suitable for some frequency ranges, and thin-walled stainless steel spheres are suitable over the whole frequency range, if they are sufficiently well made and conditions allow their deployment.